Electronic Supplementary Information (ESI) for:

Charge Separation, Recombination and Intersystem Crossing of Directly Connected Perylenemonoimide-Carbazole Electron Donor/Acceptor Dyads

Xue Zhang,[a] Ayhan Elmali,[b] Ruomeng Duan,[c] Qingyun Liu,[d] Wei Ji,[,e] Jianzhang Zhao,*[,a,f] Chen Li*[,c] and Ahmet Karatay*[,b]*

[a] State Key Laboratory of Fine Chemicals, School of Chemical Engineering, Dalian University of Technology, Dalian 116024, P.R. China. E-mail: zhaojzh@dlut.edu.cn (J. Z.)

[b] Department of Engineering Physics, Faculty of Engineering, Ankara University, 06100 Beşevler, Ankara, Turkey. Email: Ahmet.Karatay@eng.ankara.edu.tr (A.K.)

[c] School of Environment and Civil Engineering, Dongguan University of Technology, No. 1, Daxue Rd., Songshan Lake, Dongguan, Guangdong Province, P. R. China. E-mail: lichen@dgut.edu.cn (C. L.)

[d] College of Chemical and Environmental Engineering, Shandong University of Science and Technology, Qingdao 266590, P. R. China.

[e] School of Chemistry, Dalian University of Technology, Dalian 116024, P.R. China. E-mail: jiwei@dlut.edu.cn (W. J.)

[f] School of Chemistry and Chemical Engineering, and Key Laboratory of Energy Materials Chemistry, Institute of Applied Chemistry, Xinjiang University, Urumqi 830046, P. R. China

Contents

1. General Information and Synthesis

All the chemicals used in synthesis are analytically pure and were used as received, the solvents were dried and distilled before synthesis. ^{1}H and ^{13}C NMR spectra were recorded on the Bruker Avance spectrometers (400 MHz or 500 MHz). The mass spectra were measured by MALDI–TOF–HRMS spectrometer.

Compound PMI-Cz-1. Under the protection of nitrogen, the compound **PMI-Br** (0.2 mmol, 112.1 mg) and 9-phenyl-9*H*-carbazole-3-boronic acid (0.24 mmol, 68.9 mg) were added into a dry 25 ml two-necked round bottom flask, followed by adding DMF (5 ml) and water (1 ml), the nitrogen was bubbling into the system for 10 minutes, $Pd(PPh_3)_4$ (0.01 mmol, 11.5 mg) and K_2CO_3 (0.72 mmol, 100 mg) were added. The reaction was stirred at 80 °C under N_2 for 1 hour, and monitored by TLC. The mixture was cooled to room temperature and diluted with dichloromethane (30 mL), then the solution was washed with brine three times (3 × 50 mL), organic layer was dried over anhydrous sodium sulfate. After that, the dichloromethane was removed by a rotary evaporation apparatus, and the obtained crude product was purified by a column chromatography (silica gel, dichloromethane: *n*-hexane = 1:1, v/v) to get amaranthine powder (96.0 mg, yield: 66%). Mp: > 250 °C. ^{1}H NMR ($CDCl_3$, 400 MHz): δ 8.68 (d, 2H, *J* = 8.0 Hz), 8.57–8.48 (m, 4H), 8.32 (s, 1H), 8.20–8.15 (dd, 2H, *J* = 8.0 Hz), 7.74 (d, 1H, *J* = 8.0 Hz), 7.67–7.59 (m, 8H), 7.49–7.47 (m, 3H), 7.35 (d, 3H, *J* = 8.0 Hz), 2.83–2.76 (m, 2H), 1.20 (d, 12H, *J* = 8.0 Hz). ^{13}C NMR ($CDCl_3$, 126 MHz): δ 164.0, 147.6, 144.4, 141.5, 140.6, 137.9, 137.8, 137.6, 133.2, 132.1, 132.1, 131.6, 131.2, 130.7, 130.0, 130.0, 129.4, 128.8, 128.5, 128.1, 128.1, 127.8, 127.2, 127.0, 127.0, 126.5, 124.0, 124.0, 123.7, 123.2, 121.8, 120.9, 120.7, 120.5, 120.3, 120.3, 120.0, 110.1, 109.9, 77.3, 77.0, 76.8, 29.7, 29.2, 24.0, 19.7. MALDI–TOF–HRMS: Calcd [$C_{52}H_{38}N_2O_2 + H^+$], *m*/*z* = 723.2933; found, *m*/*z* = 723.2985.

Compound PMI-Cz-2. Under the protection of nitrogen, the compound **PMI-Br** (0.2 mmol, 112.1 mg) and 4-(9H-Carbozol-9-yl)phenylboronic acid (0.24 mmol, 68.9 mg) were added into a dry 25 ml two-necked round bottom flask, followed by adding DMF (5 ml) and water (1 ml), the nitrogen was bubbling into the system for 10 minutes, $Pd(PPh_3)_4$ (0.01 mmol, 11.5 mg) and K_2CO_3 (0.72 mmol, 100 mg) were added. The reaction was stirred at 80 °C under N_2 for 1 hour, and monitored by TLC. The mixture was cooled to room temperature and diluted with dichloromethane (30 mL), then the solution was washed with brine three times (3×50 mL), organic layer was dried over anhydrous sodium sulfate. After that, the dichloromethane was removed by a rotary evaporation apparatus, and the obtained crude product was purified by a column chromatography (silica gel, dichloromethane: *n*-hexane = 1:1, v/v) to get orange powder (117.2 mg, yield: 81%). Mp: > 250 °C.

^{1}H NMR ($CDCl_3$, 400 MHz): δ8.70 (d, 2H, J = 8.0 Hz), 8.60–8.52 (m, 4H), 8.21–8.16 (m, 3H), 7.80–7.71 (m, 6H), 7.60 (d, 2H, J = 8.0 Hz), 7.50–7.48 (dd, 3H, J = 8.0 Hz), 7.36 (d, 4H, J = 8.0 Hz), 2.84–2.76 (m, 2H), 1.20 (d, 12H, J = 6.0 Hz). ^{13}C NMR ($CDCl_3$, 126 MHz): δ164.0, 145.7, 142.4, 140.8, 138.8, 137.4, 132.7, 132.1, 131.5, 131.1, 130.6, 129.6, 129.5, 129.2, 128.9, 128.5, 128.5, 127.3, 127.1, 127.0, 126.1, 124.1, 124.0, 123.6, 123.6, 121.1, 121.1, 120.5, 120.2, 109.8, 77.3, 77.0, 76.8, 29.7, 29.2, 24.0. MALDI–TOF–HRMS: Calcd [$C_{52}H_{38}N_2O_2$ + H^+], m/z = 723.2933; found, m/z = 723.3018.

2. NMR and HRMS Spectra

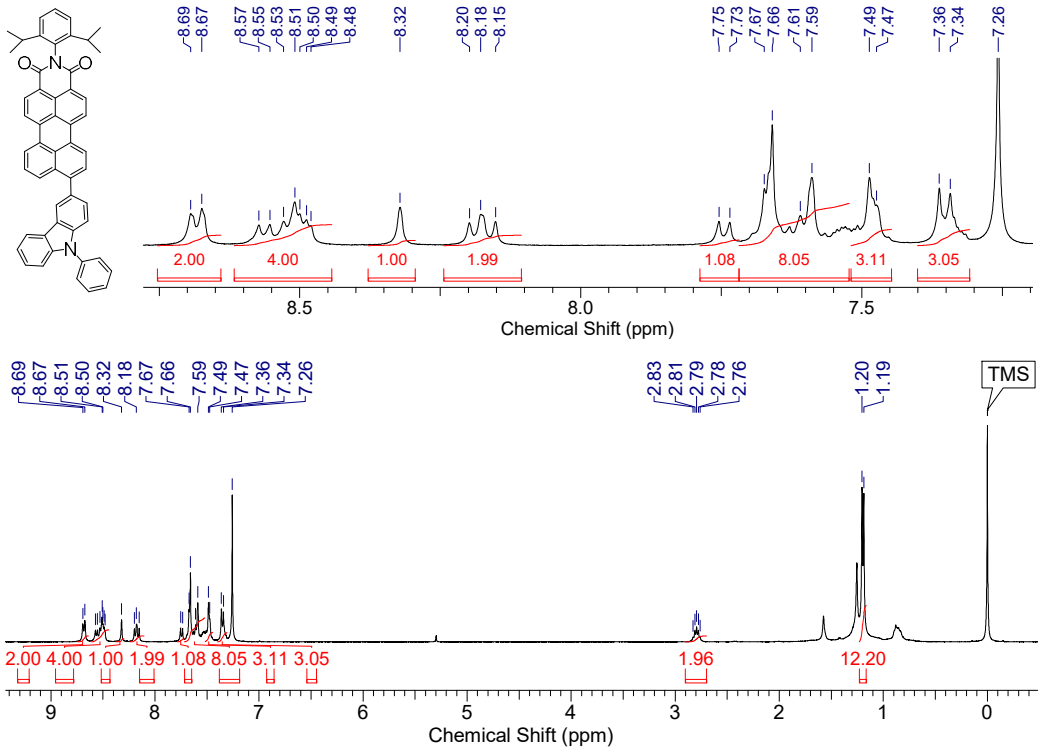

Fig. S1 ^{1}H NMR spectrum of compound **PMI-Cz-1** (400 MHz, $CDCl_3$), 25 °C.

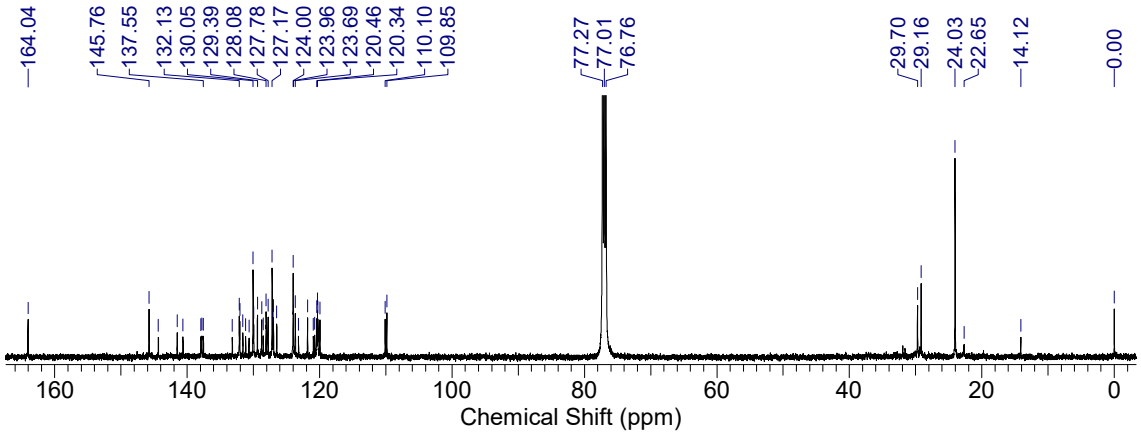

Fig. S2 ^{13}C NMR spectrum of compound **PMI-Cz-1** (126 MHz, $CDCl_3$), 25 °C.

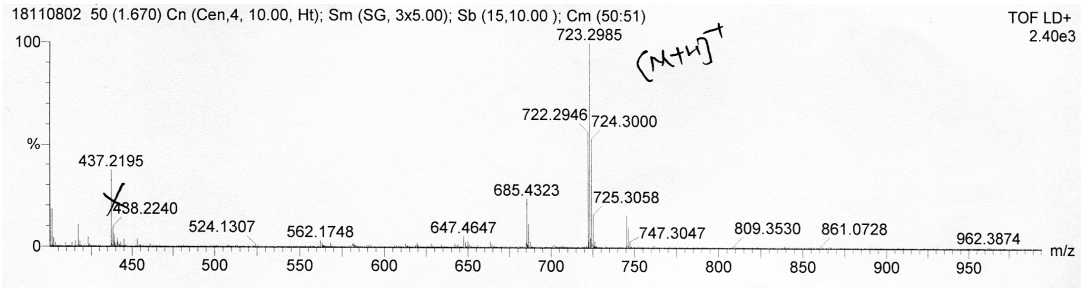

Fig. S3 MALDI–TOF–HRMS of compound **PMI-Cz-1**, 25 °C.

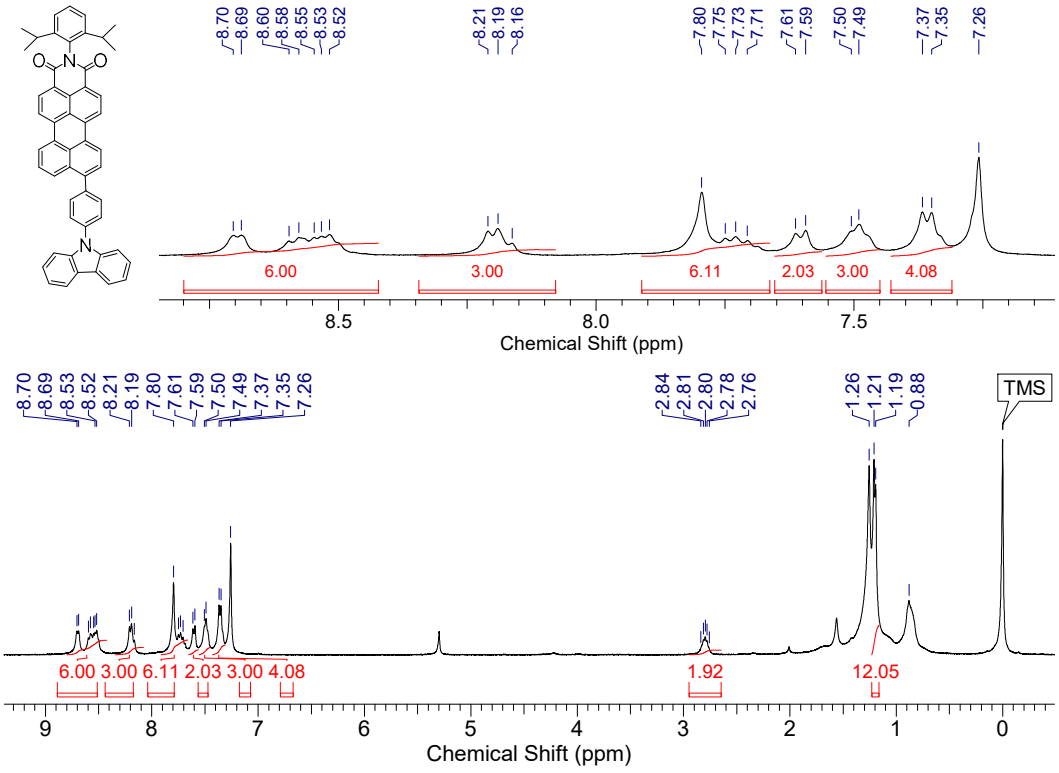

Fig. S4 ^{1}H NMR spectrum of compound **PMI-Cz-2** (400 MHz, $CDCl_3$), 25 °C.

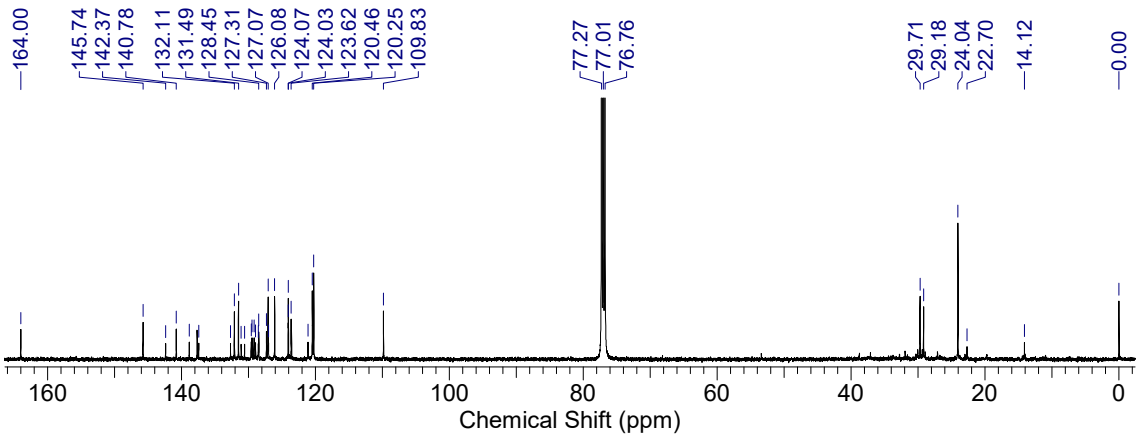

Fig. S5 ^{13}C NMR spectrum of compound **PMI-Cz-2** (126 MHz, $CDCl_3$), 25 °C.

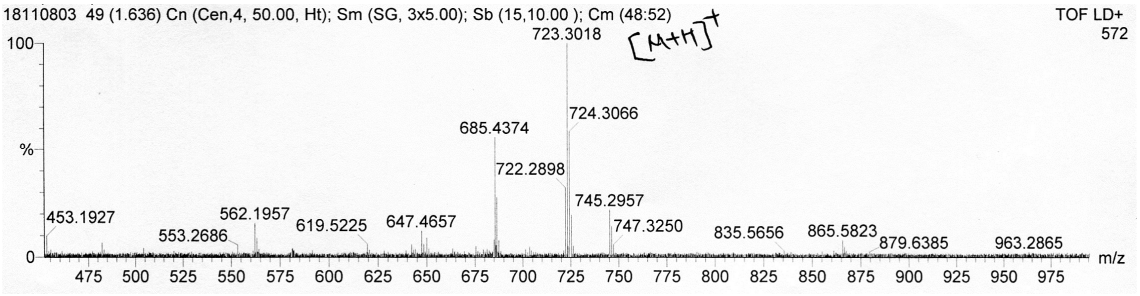

Fig. S6 MALDI–TOF–HRMS of compound **PMI-Cz-2**, 25 °C.

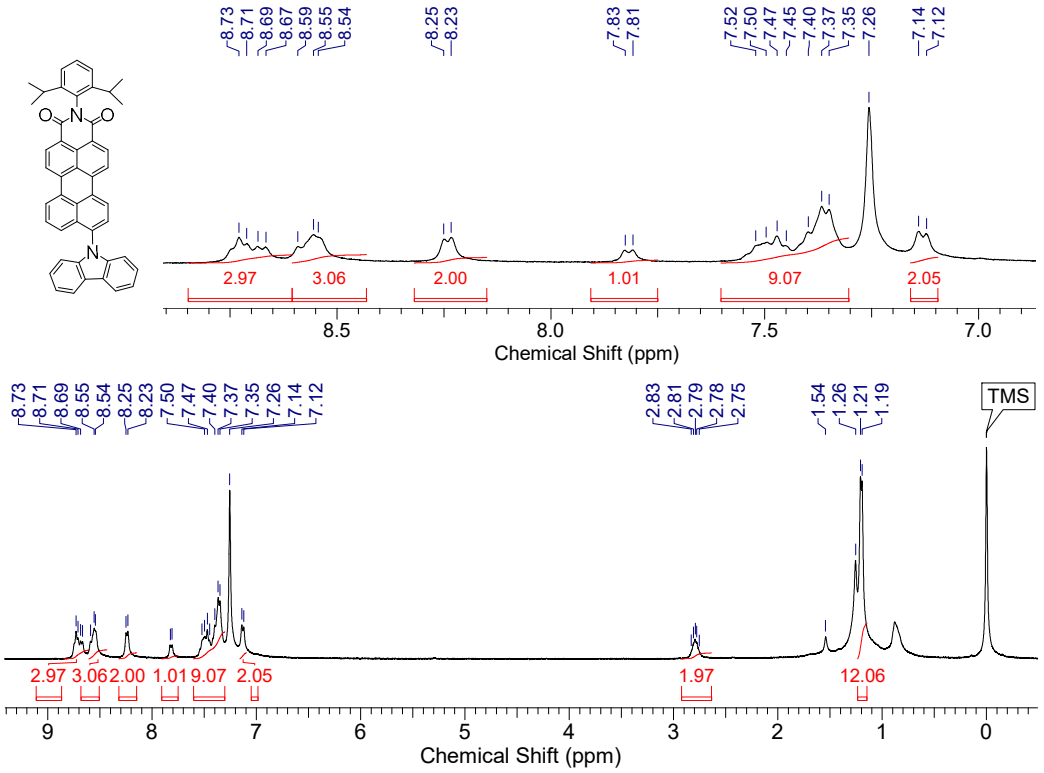

Fig S7 ^{1}H NMR spectrum of compound **PMI-Cz** (400 MHz, $CDCl_3$), 25 °C.

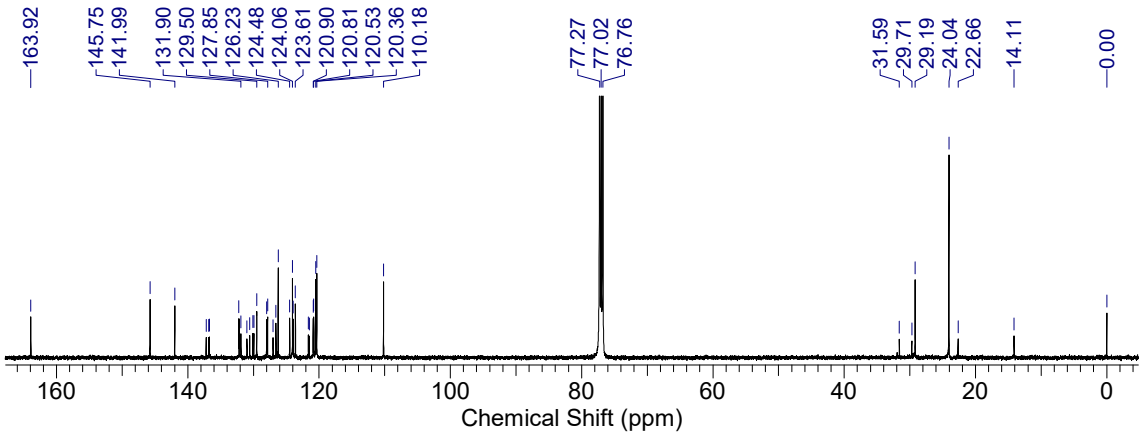

Fig. S8 ^{13}C NMR spectrum of compound **PMI-Cz** (126 MHz, $CDCl_3$), 25 °C.

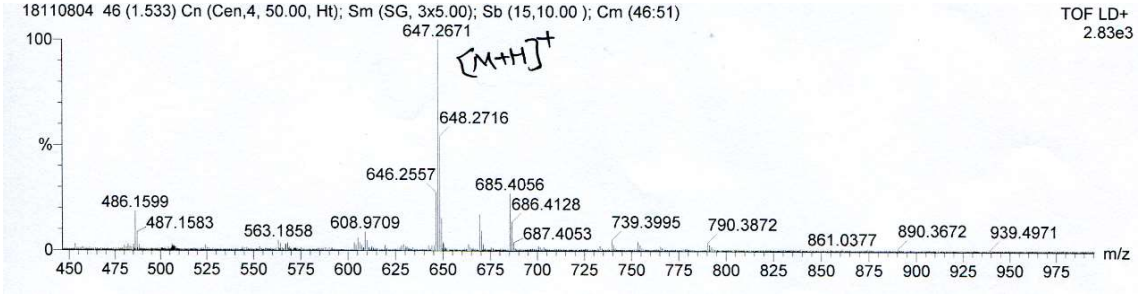

Fig. S9 MALDI–TOF–HRMS of compound **PMI-Cz**, 25 °C.

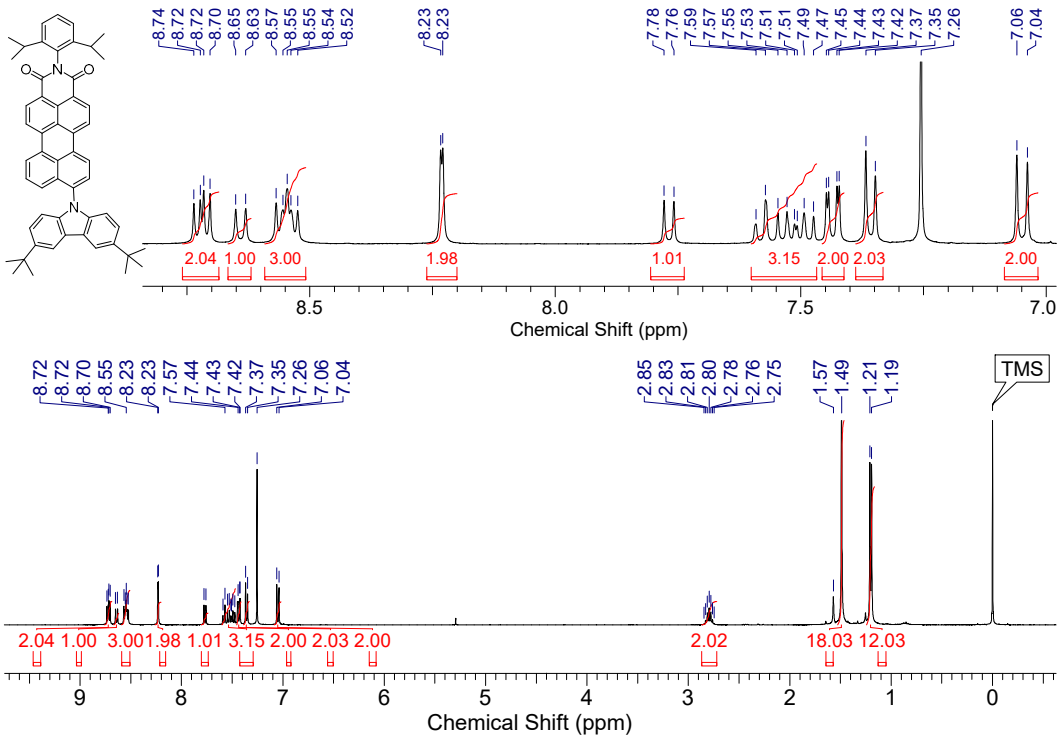

Fig. S10 ^{1}H NMR spectrum of compound **PMI-Cz-*t*Bu** (400 MHz, $CDCl_3$), 25 °C.

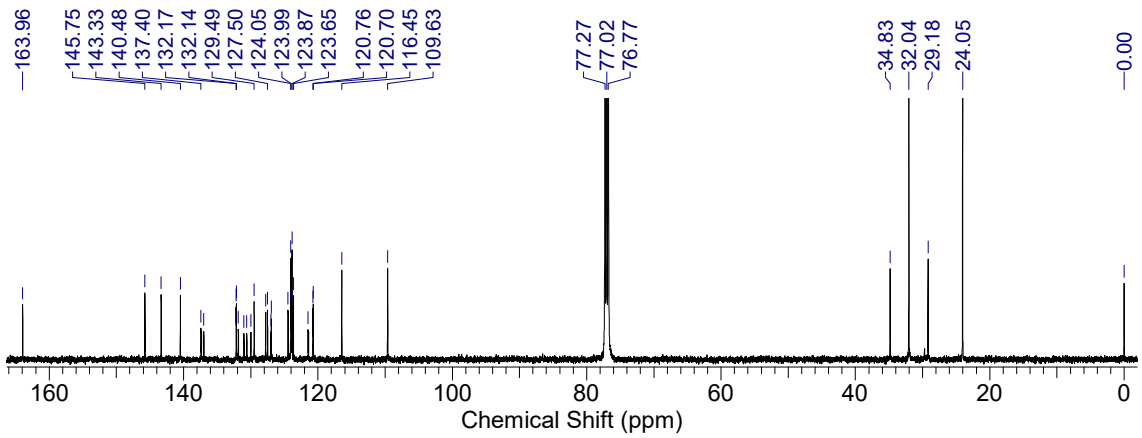

Fig. S11 ^{13}C NMR spectrum of compound **PMI-Cz-*t*Bu** (126 MHz, $CDCl_3$), 25 °C.

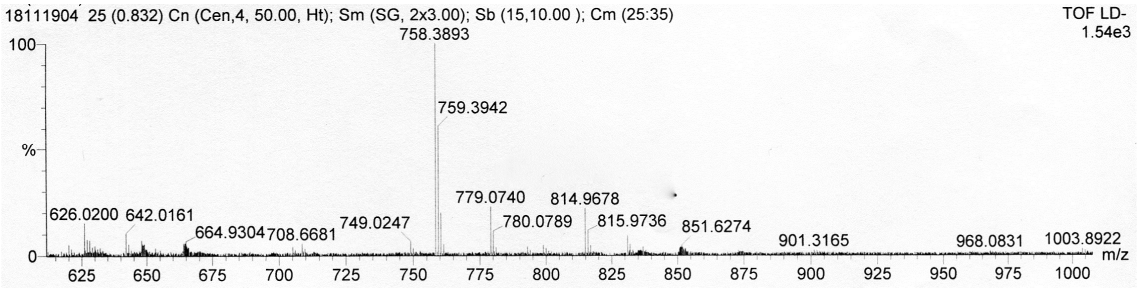

Fig. S12 MALDI–TOF–HRMS of compound **PMI-Cz-*t*Bu**, 25 °C.

3. DFT Computation.

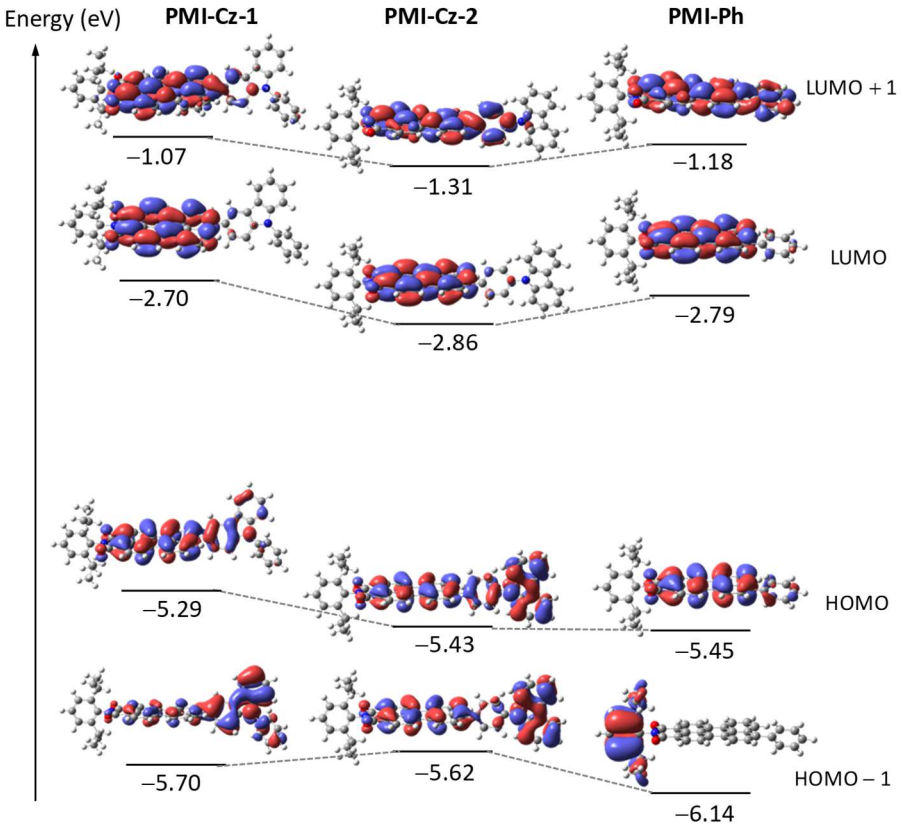

Fig. S13 Selected Frontier molecular orbitals of **PMI-Cz-1**, **PMI-Cz-2**, and **PMI-Ph** calculated by DFT (B3LYP/6-31G (d)). The energy levels of the orbits are presented (in eV).

4. UV–vis Absorption Spectra

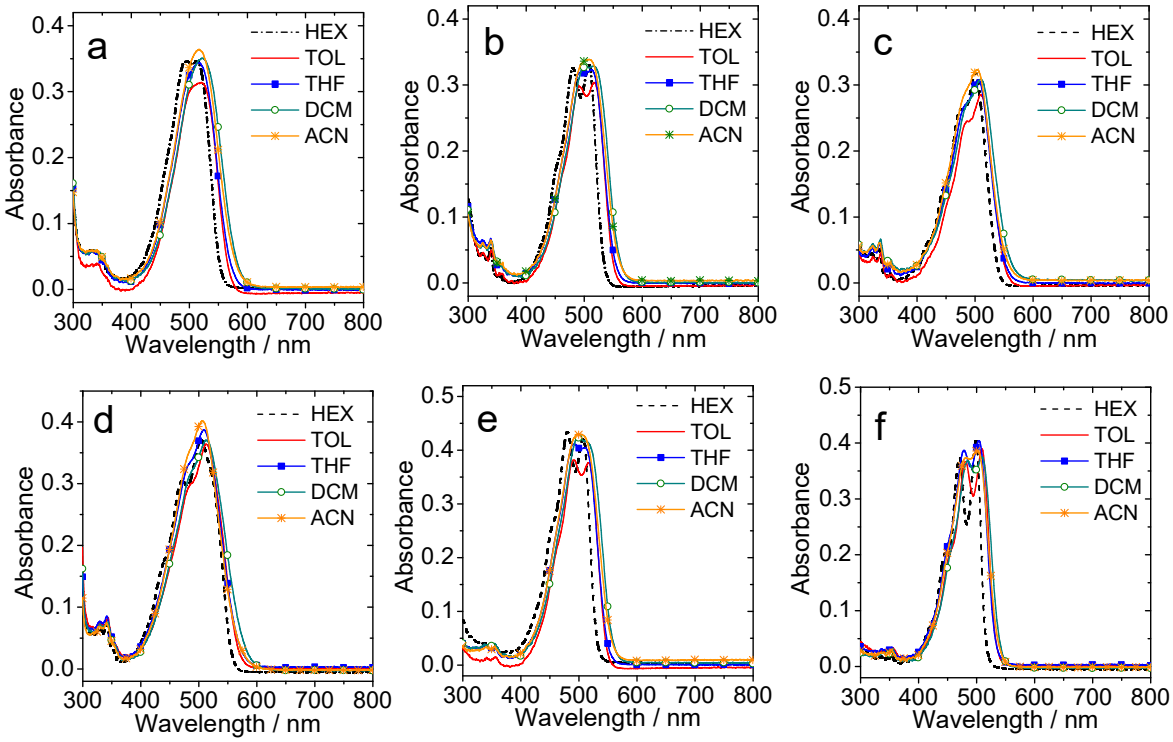

Fig. S14 UV–vis absorption spectra of (a) **PMI-Cz-1**; (b) **PMI-Cz-2**; (c) **PMI-Cz**; (d) **PMI-Cz-*t*Bu**; (e) **PMI-Ph** and (f) **PMI-Br** in different solvents. $c = 1.0 \times 10^{-5}$ M, 20 °C.

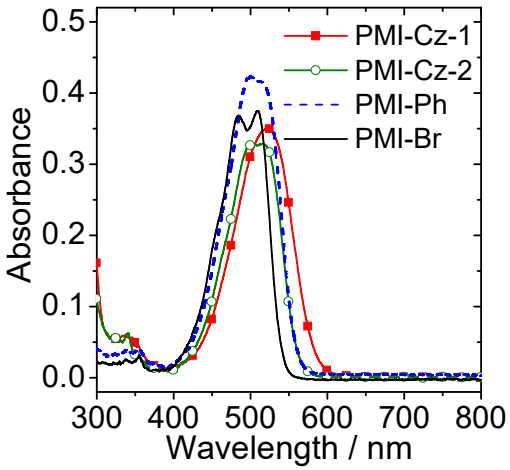

Fig. S15 UV–vis absorption spectra of the compounds in dichloromethane. $c = 1.0 \times 10^{-5}$ M, 20 °C.

5. Fluorescence Spectra

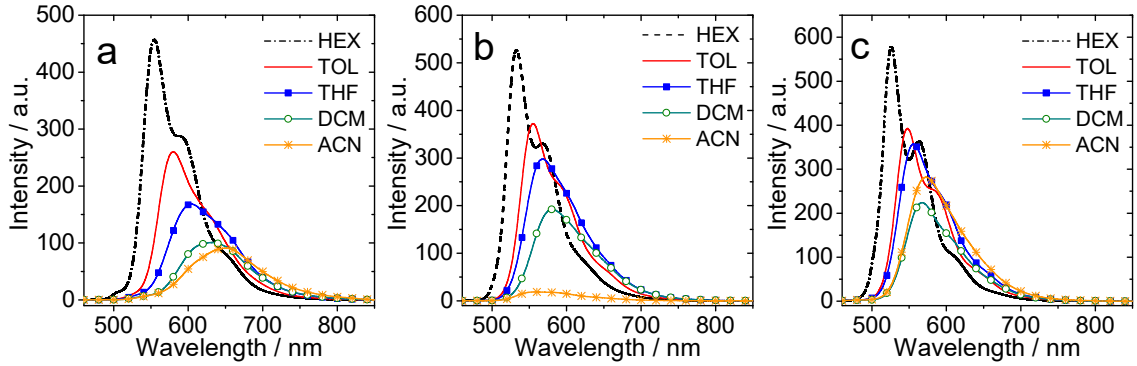

Fig. S16 Fluorescence emission spectra of (a) **PMI-Cz-1**; (b) **PMI-Cz-2** and (c) **PMI-Ph** in different solvents. Optically matched solutions were used in each panel (each of the solutions gives the same absorbance at the excitation wavelength, A = 0.100); λ_{ex} = 450 nm, 20 °C.

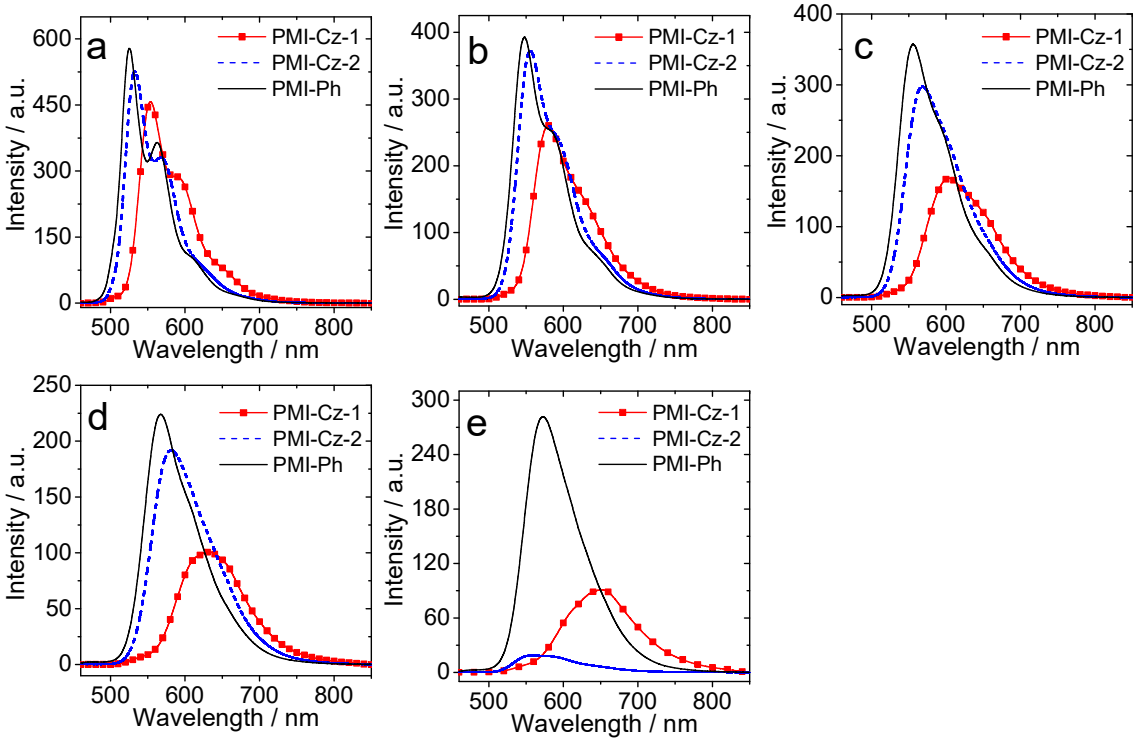

Fig. S17 Fluorescence emission spectra of the compounds in (a) *n*-hexane; (b) toluene; (c) tetrahydrofuran; (d) dichloromethane and (e) acetonitrile. Optically matched solutions were used in each panel (each of the solutions gives the same absorbance at the excitation wavelength, A = 0.100); λ_{ex} = 450 nm, 20 °C.

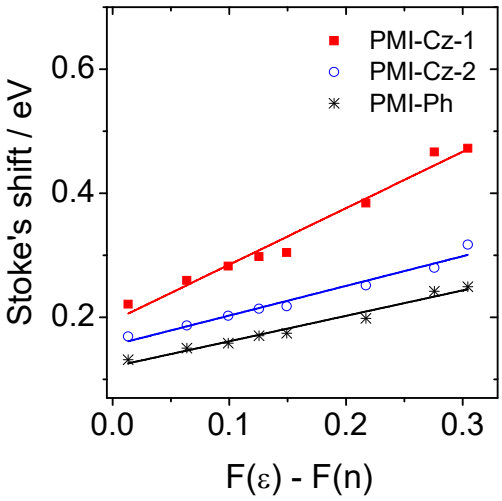

Fig. S18 Lippert-Mataga regressions of **PMI-Cz-1** (R^2 = 0.971, slope: 0.910± 0.059); **PMI-Cz-2** (R^2 = 0.965, slope: 0.478± 0.034) and **PMI-Ph** (R^2 = 0.970, slope: 0.410± 0.027).The solvents used are toluene, dichloromethane: toluene = 1 : 9 (v/v), dichloromethane: toluene = 2 : 8 (v/v), dichloromethane: toluene = 3 : 7 (v/v), chloroform, dichloromethane, N,N-Dimethylformamide and acetonitrile, 20 °C.

6. Fluorescence Lifetime

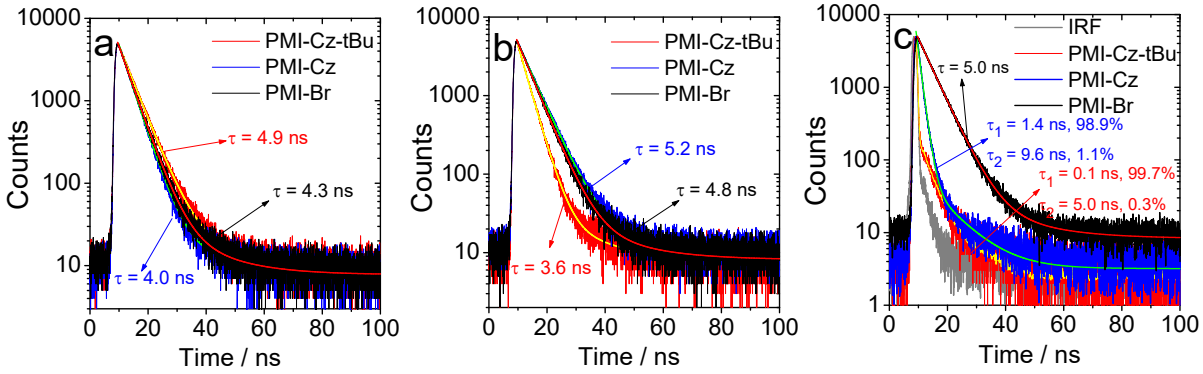

Fig. S19 Fluorescence lifetime of the compounds in (a) *n*-hexane; (b) dichloromethane and (c) acetonitrile. *c* = 1.0 × 10^{-5} M, λ_{ex} = 450 nm, 20 °C.

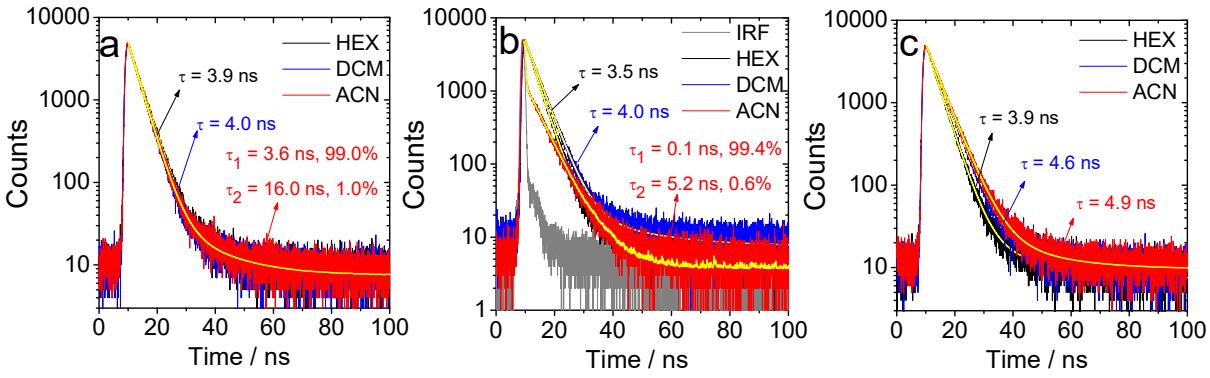

Fig. S20 Fluorescence lifetime of (a) **PMI-Cz-1** (λ_{em} = 550 nm in *n*-hexane; λ_{em} = 630 nm in dichloromethane; λ_{em} = 650 nm in acetonitrile); (b) **PMI-Cz–2** (λ_{em} = 540 nm in *n*-hexane; λ_{em} = 580 nm in dichloromethane; λ_{em} = 560 nm in acetonitrile) and (c) **PMI-Ph** (λ_{em} = 520 nm in *n*-hexane; λ_{em} = 570 nm in dichloromethane; λ_{em} = 570 nm in acetonitrile) in different solvents. $c = 1.0 \times 10^{-5}$ M, λ_{ex} = 450 nm, 20 °C

7. Electrochemical Measurement

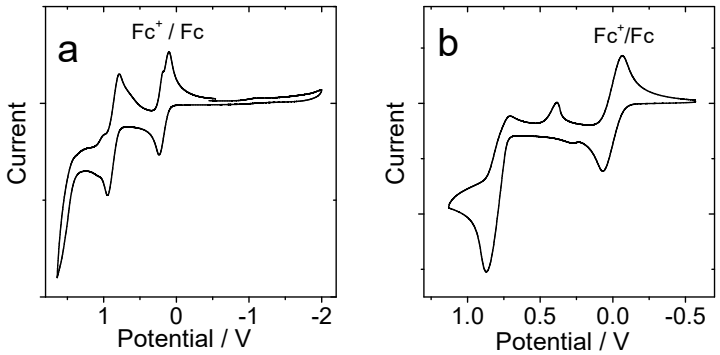

Fig. S21 Cyclic voltammograms of (a) **Cz-*t*Bu** and (b) **Carbazole** in deaerated dichloromethane containing 0.05M $Bu_4N[PF_6]$ as supporting electrode and $Ag/AgNO_3$ as reference electrode. Scan rate: 100 mV/s. Ferrocene (Fc) was used as internal reference (set as 0 V in the cyclic voltammograms), $c = 5.0 \times 10^{-4}$M, 20 °C.

For eqn (4)–(6), ΔG_{CS} is the Gibbs free-energy change of charge separation process, e is the charge of a single electron, E_{RED} and E_{OX} are the half-wave potential for one-electron reduction and oxidation of the electron-acceptor unit, respectively, E_{00} represent the energy level approximated with the crossing point of UV−Vis absorption and fluorescence emission after normalization at the singlet excited state. ΔG_S is the static coulombic energy, ε_S is the static dielectric constant of the solvent, ε_0 is the permittivity of free space, R_{CC} is the center-to-center separation distance between the electron donor and acceptor determined by optimized conformation by DFT calculation, R_D and R_A are the radius of electron donor and acceptor, ε_{REF} is the static dielectric constant of the solvent used for the electrochemical studies and E_{CS} is charge separation state energy level.

8. Femtosecond Transient Absorption Spectroscopy.

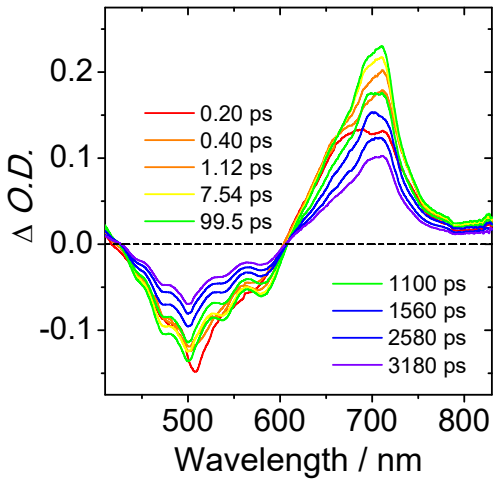

Fig. S22 Femtosecond time-resolved transient absorption spectra of **PMI-Cz** at different time delays in *n*-hexane. λ_{ex} = 500 nm. c = 1.0 × 10^{-5} M. 20 °C.

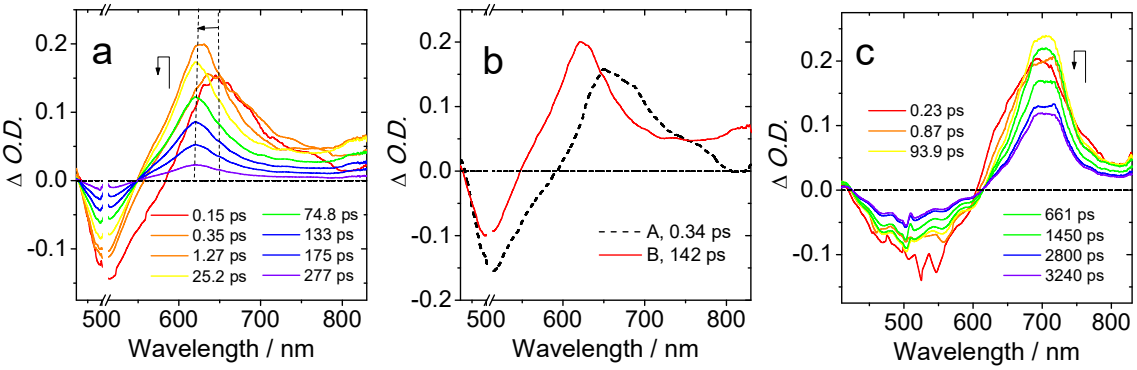

Fig. S23 (a) Femtosecond time-resolved transient absorption spectra of **PMI-Cz-*t*Bu** at different time delays in acetonitrile. (b) Related species-associated difference spectrum (SADS) obtained from global analysis. (c) Femtosecond time-resolved transient absorption spectra of **PMI-Cz-*t*Bu** in *n*-hexane. λ_{ex} = 500 nm. c = 1.0 × 10^{-5} M. 20 °C.

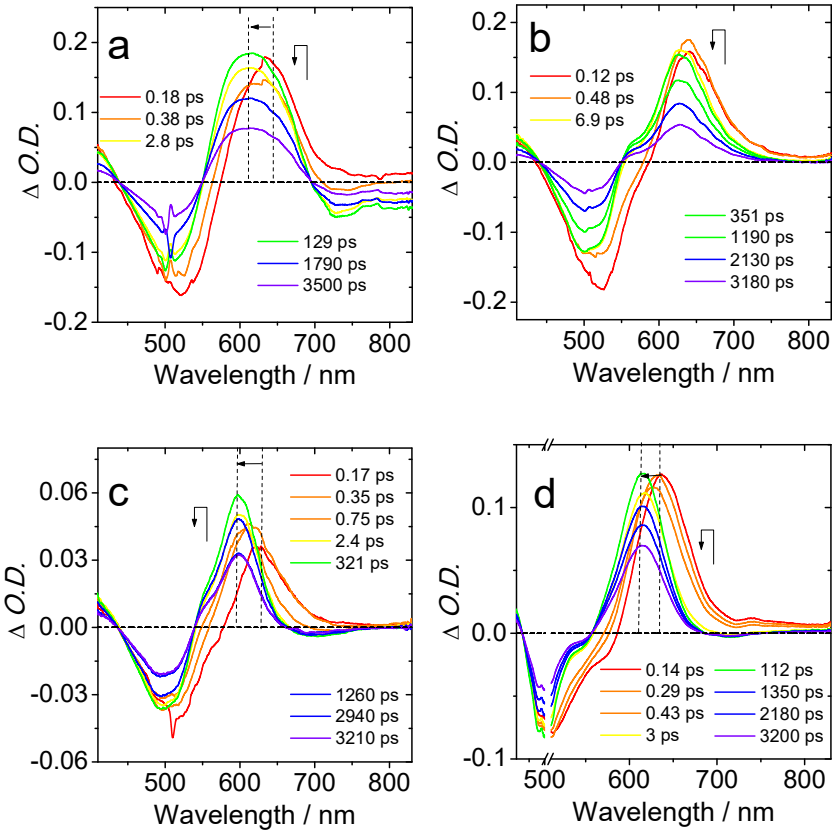

Fig. S24 Femtosecond time-resolved transient absorption spectra of (a) **PMI-Cz-1**, (b) **PMI-Cz-2**, (c) **PMI-Ph** and (d) **PMI-Br** at different time delays in acetonitrile. λ_{ex} = 500 nm. c = 1.0 × 10^{-5} M. 20 °C.

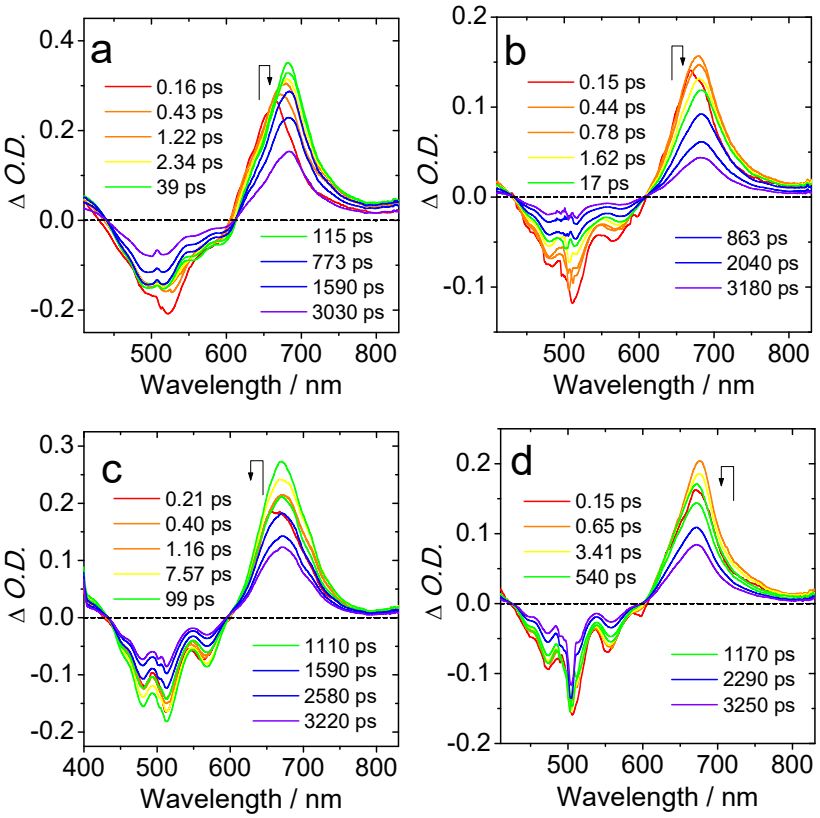

Fig. S25 Femtosecond time-resolved transient absorption spectra of (a) **PMI-Cz-1**, (b) **PMI-Cz-2**, (c) **PMI-Ph** and (d) **PMI-Br** at different time delays in *n*-hexane. λ_{ex} = 500 nm. c = 1.0 × 10^{-5} M. 20 °C.

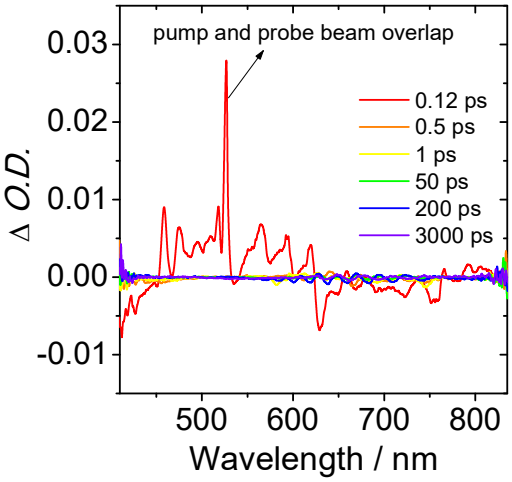

Fig. S26 Femtosecond time-resolved transient absorption spectra of acetonitrile. λ_{ex} = 500 nm. 20 °C.

9. Simplified Jablonski Diagram

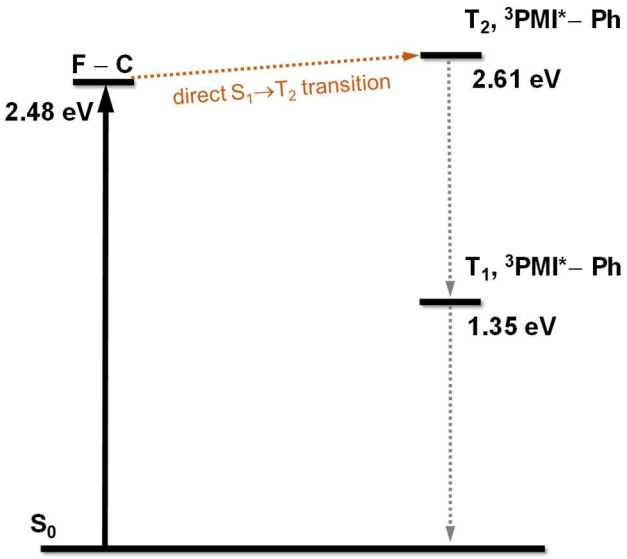

Fig. S27 Simplified Jablonski diagram illustrating the photophysical processes involved in **PMI-Ph** upon photoexcitation**:** The energy levels of the excited state are derived from the DFT calculation. The number of the superscript designates the spin multiplicity of the states. F-C stands for the Franck-Condon state.

10. Photoreduction Experiment

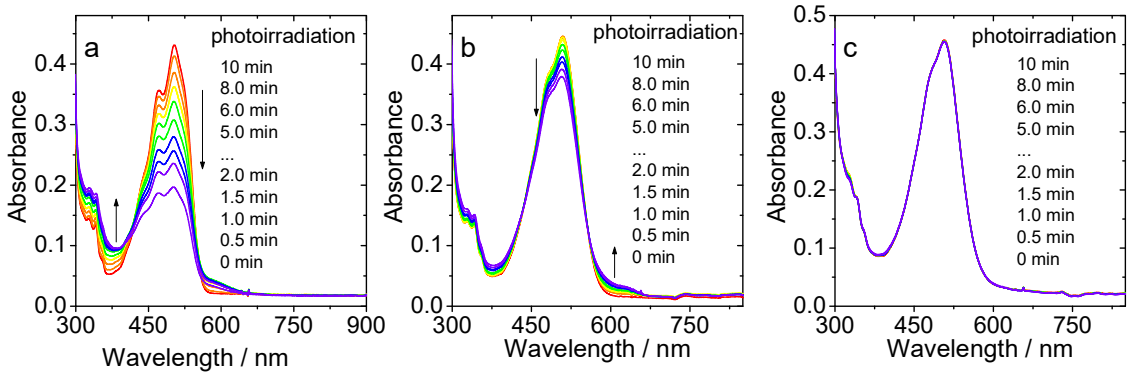

Fig. S28 UV−vis absorption spectra of **PMI-Cz-*t*Bu** in the presence of triethylamine in N_2 radiated by Xe lamp (a) in *n*-hexane, (b) in tetrahydrofuran, (c) in acetonitrile. *c* [PMI-Cz-*t*Bu] = 1.0×10^{-5} M; *c* [TEA] = 3.3×10^{-2} M, 20 °C.

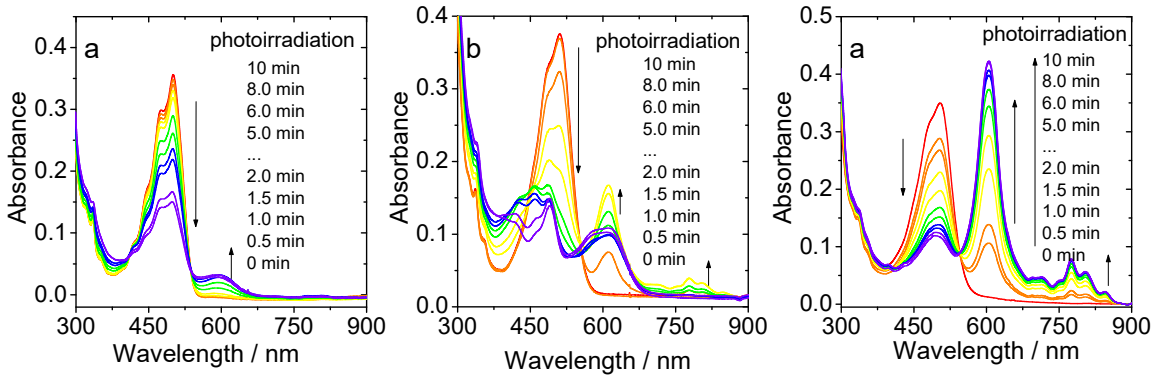

Fig. S29 UV−vis absorption spectra of **PMI-Cz** in the presence of triethylamine in N_2 radiated by Xe lamp (a) in *n*-hexane, (b) in dichloromethane, (c) in acetonitrile. *c* [PMI-Cz] = 1.0×10^{-5} M; *c* [TEA] = 3.3×10^{-2} M, 20 °C.

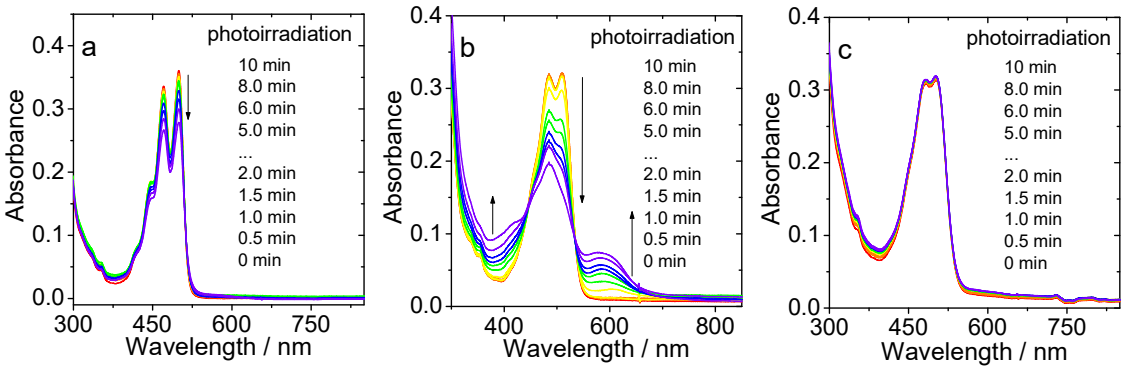

Fig. S30 UV−vis absorption spectra of **PMI-Br** in the presence of triethylamine in N_2 radiated by Xe lamp (a) in *n*-hexane, (b) in dichloromethane, (c) in acetonitrile. *c* [PMI-Br] = 1.0×10^{-5} M; *c* [TEA] = 3.3×10^{-2} M, 20 °C.